



Enhanced weathering leads to substantial C accrual on crop macrocosms

- François Rineau^{*1}, Alexander H. Frank^{2,3}, Jannis Groh^{4,5,6}, Kristof Grosjean¹, Arnaud Legout⁷, Daniil I. Kolokolov⁸, Michel Mench⁹, Maria Moreno-Druet¹, Benoît Pollier⁷, Virmantas Povilaitis¹⁰, Johanna Pausch¹¹, Thomas Puetz⁵, Tjalling Rooks¹, Peter Schröder¹², Wiesław Szulc¹³, Beata Rutkowska¹³, Xander Swinnen¹, Sofie Thijs¹, Harry Vereecken⁵, Janna V. Veselovskaya⁸, Mwahija Zubery¹, Renaldas Žydelis¹⁰, Evelin Loit¹⁴
- ¹Environmental Biology, Centre for Environmental Sciences, Hasselt University, Diepenbeek, Belgium.
²Center of Stable Isotope Research in Ecology and Biogeochemistry (BayCenSI), BayCEER, University of Bayreuth, Universitätsstr. 30, 95445 Bayreuth, Germany
³Department of Plankton and Microbial Ecology, Leibniz Institute of Freshwater Ecology and Inland Fisheries (IGB), Zur alten Fischerhütte 2, 16775 Stechlin, Germany
⁴Department of Soil Science and Soil Ecology, Institute of Crop Science and Resource Conservation, University of Bonn, Bonn, Germany
⁵Agrosphere Institute (IBG-3), Forschungszentrum Jülich (FZJ), Jülich, Germany
⁶Isotope Biogeochemistry and Gas Fluxes, Research Area 1 “Landscape Functioning”, Leibniz Centre for Agricultural Landscape Research (ZALF), Müncheberg, Germany
⁷INRAE, BEF, F-54000 Nancy, France
⁸Boriskov Institute of Catalysis, Novosibirsk, Ac. Lavrentiev av. 5, Novosibirsk 630090, Russia
⁹Univ. Bordeaux, INRAE, Biogeco, Bat B2, Allée G. St-Hilaire, F-33615 Pessac cedex, France
¹⁰Institute of Agriculture, Lithuanian Research Centre for Agriculture and Forestry, Lithuania
¹¹Agroecology, BayCEER, University of Bayreuth, Universitätsstr. 30, 95445 Bayreuth, Germany
¹²Helmholtz Center Munich, Research Unit Environmental Simulation, Ingolstädter Landstrasse 1, D-85764 Neuherberg
¹³Institute of Agriculture, Warsaw University of Life Sciences, Nowoursynowska 166, 02-787 Warsaw, Poland
¹⁴Estonian Univ Life Sci, Inst Agr & Environm Sci, Tartu, Estonia

Correspondence to: François Rineau (francois.rineau@uhasselt.be)



Abstract. Enhanced weathering (EW) is proposed as a key strategy for climate change mitigation. It involves the application of silicate rock powder to soils, where it is expected to react with CO₂ released from soil respiration, forming stable carbonate ions and thereby sequestering carbon. Here, we evaluated the effects of EW on a crop ecosystem within a macro-scale ecotron—an enclosed facility enabling complete quantification of carbon fluxes among the atmosphere, vegetation, soil, and leachates. EW treatment resulted in an almost three-fold enhancement of measured carbon flux into the soil, achieving rates up to 1.5 tons per hectare. Furthermore, the magnitude of carbon sequestration exceeded what could solely be attributed to electrochemical transformations. Therefore, we conclude that EW facilitated significant carbon accrual in our simulated ecosystems via not only carbonate precipitation but also enhanced biogeochemical activities promoting additional carbon storage. Based on these findings, we speculate on the underlying pathways responsible for such outcomes.

1 Introduction

Agricultural systems are responsible for approximately 11% of anthropogenic CO₂ emissions (IPCC, 2014), highlighting the urgent need for scalable mitigation strategies to meet the CO₂ reduction targets of the 2015 Paris Agreement. Enhanced rock weathering (EW) has emerged as a promising approach in this context (Beerling et al., 2020). The method involves applying silicate rock dust to soils, where it reacts with CO₂ from soil respiration to form bicarbonate and carbonate ions. Theoretically, these carbonates may either remain in the soil or be leached into groundwater and transported to aquatic systems, where they could help reduce ocean acidification—both pathways contributing to carbon sequestration. Early studies support some of these theoretical predictions (Dietzen & Rosing, 2023; Guo et al., 2023; Rijnders et al., 2023), suggesting that EW could be implemented across large agricultural areas. Its carbon removal potential is estimated at 0.5 to 4 Gt CO₂ per year (Beerling et al., 2020), with additional benefits for soil health in nutrient-poor soils (Beerling et al., 2018). However, significant uncertainties remain—particularly for agricultural soils (Cipolla et al., 2021)—underscoring the need for robust experimental validation. Field experiments have revealed important findings, such as substantial CO₂ removal from soil pore water (Holzer et al., 2023) and increased inorganic carbon accumulation (Kantola et al., 2023). However, the open nature of field settings complicates comprehensive tracking of ecosystem carbon fluxes, especially the fate of carbonate ions. Mesocosm studies, while more controlled, have often lacked sufficient soil depth (<70 cm), potentially missing important processes occurring deeper in the soil profile (Vienne et al., 2022). To address these limitations, we conducted an EW amendment experiment on an oat cropping system within an ecotron—a controlled, closed-environment facility that enables real-time monitoring of



55 ecosystem-level carbon fluxes (Roy et al., 2021). This setup allowed for a direct test of the hypothesis that basalt application leads to carbonate formation and long-term carbon storage.

2 Material and Methods (as Heading 1)

2.1 Ecotron facility

60 At the UHasselt ecotron, large (4.7m³, diameter 2 m) and deep (1.5 m) macrocosms are exposed to tightly controlled environmental treatments in gas-tight enclosures, while high-frequency measurements allow accurate estimation of the ecosystem C budget on an hourly scale (Rineau et al., 2019). This enables to study the actual dynamics of the process of EW and the fate of its products in a real ecosystem, while the large macrocosms ensure a necessary degree of realism in the measured processes (Clobert et al., 2018). In short, the macrocosms were placed within a large, gas-tight chamber topped with
 65 a dome transparent to both UV and photosynthetically active radiation (PAR). Within the chamber, environmental conditions including air temperature, precipitation, relative humidity, CO₂ concentration, and wind speed were precisely controlled. Soil temperature and water tension were also regulated using a heat exchange system and a network of suction cups installed at the base of each lysimeter—the vessel containing the soil and plant macrocosm. Each lysimeter was equipped with sensors located at five soil depths (10, 20, 35, 60, and 140 cm) across three radial profiles (spaced 120° apart). These sensors continuously
 70 monitored soil temperature, water tension, volumetric water content, and electrical conductivity. Above the plant canopy, air samples were collected to monitor CO₂, CH₄, and N₂O concentrations using two gas analysis systems (LGR 911-0011 and SYNSPEC gas analyser; Envicontrol, Gembloux, Belgium). Additionally, net radiation (incoming minus outgoing radiation) was measured using pyranometers, and PAR was monitored with a LI-190R quantum sensor. All measurements were recorded at intervals ranging from once every 30 minutes to once per minute, depending on the parameter.

75 Soil water samples were collected *via* suction cups installed at 10, 20, 35, 60 and 140 cm depth and in triplicate in each lysimeter. The tension in the suction cups was adjusted by a vacuum pump (VS Pro, METER group, USA) applying a constant -50 hPa and -150 hPa to the upper (10, 20, 35 cm) and lower (60, 140 cm) cups, respectively, as upper soil layers are usually drier. The water extracted from the cups was then stored in 1L-bottles sitting in a temperature-controlled cabinet (+10 °C).



Every three weeks, the water contained in the bottles was filtered at 0.45µm and analysed for total organic Carbon (TOC),
 80 total Nitrogen (TN), anions and cations. Four water samples taken from the main pipe feeding the rain system were also filtered
 and analysed in the same way, as well as water samples from the leachate tank (aliquot of the drainage).

2.2 Macrocosms

Six large macrocosms were extracted undisturbed from a dry heathland in ‘Hoge Kempen’ National Park, Belgium, in
 November 2016 and placed in ecotron units at UHasselt. The soil in this plot is a brunic-dystric arenosol, with an organic layer
 85 of 10-20 cm depth, on top of a sandy matrix containing 5-10cm clay lenses, and with a ferric iron precipitation horizon at, 150-
 200 cm depth. The soil pH varies from 6 on the top, organic layer and 4 to 5 on the B horizon. The TOC content of the soil
 varies between 1.9% in the top, organic layer and 0.5 % below down to 140 cm. They were exposed to recreated ambient
 climate conditions until January 2020, after which they were "marginalized" by removing topsoil and vegetation to simulate
 nutrient-poor marginal land. From January 2020 to September 2022, the macrocosms were subjected to a future climate
 90 scenario (2070-2075) and agricultural treatments to mimic the conversion of heathland to crop fields. Barley was cultivated
 with foliar Si amendments (Rineau et al., 2024), followed by mustard as a cover crop, and mineral NPK fertilization was
 applied. Basalt was added to three units (10 t/ha) and incorporated into the topsoil, with all units tilled during seeding. The
 basalt was finely ground (<1mm particle size) and consisted mostly of plagioclases and pyroxenes (38 and 26%, respectively;
 for more details see Table S1). The basalt composition was moderately reactive for enhanced weathering, with relatively low
 95 olivine (7%) and moderate feldspar (10%) contents, leading to a potential C removal of a maximum possible removal of 529
 kg CO₂/t (144 kgC/t). We applied 10t/Ha, which theoretically led to a maximum of 1444 kgC/Ha of removal (Table S1). The
 soil pH at that moment was 7 in all units. Oats were then planted and harvested after 150 days. Manual weeding was carried
 out during the growing season. More details are provided in the “macrocosms details” box in the supplementary information.

2.3 Climate simulations

100 The experiment was conducted under climate conditions projected for 2070-2075 (RCP 8.5 scenario), allowing for realistic
 simulations of elevated atmospheric CO₂ levels and their effects on the ecosystem. The ecotron served as a real-time, accurate
 simulator of climate scenarios, controlling air temperature, humidity, rainfall, CO₂ concentration, wind speed, soil temperature,



and bottom soil water tension for each macrocosm. High-frequency monitoring was performed for key parameters, including photosynthetically active radiation (PAR), net radiation, lysimeter weight, leachate weight, and concentrations of CH₄ and N₂O. Soil water samples were collected at five separate depths and in triplicate for chemical analysis. More details about the ecotron technicalities can be found in (Rineau et al., 2019; Roy et al., 2021). Climate data were downscaled to a half-hourly resolution using projections based on local climate models (more details in (Vanderkelen et al., 2019)), and CO₂ levels were adjusted to reflect future increases by adding a 221ppm offset to real-time measurements from a nearby ICOS station. The characteristics of the climatic conditions applied to the six macrocosms are shown in Figure S1. The crops were exposed to a climatic year typical of what is expected in 2070 according to local projections of the IPCC 8.5 scenario (Vanderkelen et al., 2019).

2.4 Plant biomass

The quantification of plant biomass was conducted to assess the influence of basalt amendment on vegetation development as well as to estimate the overall carbon balance within the ecosystem. At harvest, plant density was measured using three 50 x 50 cm quadrats per macrocosm. In each quadrat, oat stems were counted, and five plants (shoot and root) were randomly sampled for biomass. Plants were dried at 60°C, and dry weights of grains, chaff, stems, leaves, and roots were measured, along with the number of grains and leaves. Yield was calculated based on plant density and grain weight per unit area. Carbon content in oat biomass was estimated by multiplying the dry weight of plant organs by stem density, assuming a 40% carbon content (Sun et al., 2019). For weeds (primarily *Rumex acetosella*), biomass was measured after manual removal, corrected for water content, and scaled to the lysimeter area, also assuming a 40% carbon content. Note that we tested the sensitivity of our results to this C content assumptions, see the statistics section below.

2.5 CO₂-C net flux

Silicate rock amendments are of interest due to their potential to increase ecosystem carbon (C) sequestration. To verify this, we estimated C sequestration in both plant biomass and soil by measuring net CO₂-C and CH₄-C fluxes. Net CO₂-C flux, the largest component, was calculated as the exchange between the atmospheric compartment and each macrocosm. CO₂ concentrations in each chamber were maintained to mimic future levels (ambient + 221 ppm offset) by automated CO₂ gas



injection or scrubbing by extracting air from the chamber and passing it through a lime-filled container. The CO₂ levels were measured every 30 minutes by the means of an air sampler located 1m above the macrocosm's soil surface. The air sample is then conducted to a Synspec gas analyser where its CO₂ concentration is measured using gas chromatography. Given the airtight nature of the chambers and the established relationship between CO₂ changes and injection or scrubbing time, we estimated the net CO₂-C stored or released over time. Fluxes were calculated every 30 minutes and converted to daily rates (g CO₂-C/m²) using the ideal gas law (air temperature on top of the macrocosm as well as air pressure are measured automatically). Data gaps were filled using a moving average function (ALMA function from the TTR package in R). Interventions in the chambers can slightly disturb the system's carbon balance, as CO₂ levels in the chamber equilibrate with those of the main corridor. However, given the large chamber volume, we estimate that even a doubling of CO₂ concentration from 400 to 800ppm—assuming all additional carbon were taken up by the plants—would result in only about 50 mg of additional sequestered carbon per intervention. Over the entire experiment, this would amount to a maximum of approximately 1 g per unit, which is too little to affect the main conclusions of this study. Furthermore, the number of interventions was evenly distributed across units, ensuring that this effect was consistent between both treatments.

2.6 CH₄-C net flux

The net CH₄-C flux was determined as the exchange of CH₄-C between the atmospheric compartment and the macrocosm. CH₄ concentrations in the growth chambers were measured every 30 minutes using a Los Gatos Research (LGR) gas analyzer. Previous measurements confirmed that methane concentrations remained stable in the absence of a macrocosm and were unaffected by CO₂ scrubbing, but fluctuated rapidly when the chamber doors were opened. These events were therefore identified and corrected for in the flux calculations. Additional tests verified that CH₄ fluxes were not influenced by microbial activity in the drainage system. The CH₄ budget was computed by correcting the CH₄ concentration changes for door-opening artefacts, then converting the resulting values from ppm to g CH₄-C m⁻² day⁻¹ using the ideal gas law, methane's carbon fraction (75%), and recorded chamber temperature and pressure.



2.7 Rainwater C flux

150 The amount of carbon (C) added to each macrocosm through simulated rainfall was estimated by multiplying the average non-purgeable organic carbon concentration in the irrigation water—based on triweekly measurements—with the cumulative precipitation over each corresponding three-week period. Precipitation amounts were estimated using the AWAT model (Hannes et al., 2015; Peters et al., 2017), following the approach described in (Rineau et al., 2024). These values were then aggregated for each macrocosm by summing the contributions over the entire growing season.

155 2.8 Leachate C flux

We estimated the amount of C leaching out of the macrocosm using the following calculation:

$$leachateC = leachate \times soil\ waterC$$

"Leachate" refers to the cumulative volume of water collected in each unit's weighable leachate tank during the three-week
160 intervals between sampling events, while "soil water C" denotes the average non-purgeable organic carbon concentration in the soil water samples collected at each sampling date. Based on prior experience, the values exceeding 50 mg/L were considered outliers and excluded from the calculations. Final values were aggregated by summing the carbon fluxes per unit over the entire growing season.

2.9 Sampling C flux

165 Some of the macrocosm C has also been exported through soil water sampling throughout the experiment. To account for this, we used the following calculation:

$$samplingC = 10 \times 12 \times average\ C$$

Where 10 corresponds to the average amount of water collected per unit per sampling campaign (10 l in every unit); 12 is the number of sampling campaigns during the experiment; and "average C" is the average non-purgeable concentration in this unit
170 throughout all samplings. The obtained values are therefore a C flux aggregated through the whole growing season.



2.10 Soil C net flux

In the previous sections, we described the measurements of the following fluxes: CO₂-C net flux, CH₄-C net flux, rainwater-C flux, leachate C flux, sampling C flux, and plant biomass C production. The only unknown flux needed to close up the C budget of the ecosystem is then soil C net flux, that was calculated as follows:

$$175 \quad \text{soilC} = \text{CO}_2\text{C} + \text{CH}_4\text{C} + \text{rainfallC} - \text{plantC} - \text{leachateC} - \text{samplingC}$$

Where “soilC” is the soil C net flux; “CO₂C” is the CO₂-C net flux (negative if the macrocosm was a net sink of CO₂-C); CH₄C is the CH₄-C net flux (negative if the macrocosm was a net sink of CH₄-C); rainfallC the rainwater-C flux; plant-C is plant biomass C (positive), leachateC the leachate C flux and samplingC the sampling C flux. Since plant biomass was measured only once, at harvest, carbon fluxes could only be estimated as integrated values over the entire growing season.

180 Consequently, all related data were aggregated across the full experimental period (01/03/2022–01/09/2022). The net CO₂-C flux inherently accounts for both photosynthetic uptake and respiratory losses, and we were not able to differentiate between the two.

2.11 Soil C pools

To assess if EW resulted in the formation of inorganic C, we estimated the size of the different organic and inorganic C pools (dissolved organic C: DOC, dissolved inorganic C: DIC, particulate organic C: POC and particulate inorganic C: PIC). We monitored DIC by measuring the sum of carbonates, bicarbonates, and carbonic acid and DOC by measuring non-purgeable organic C in soil pore water collected from five depths (10, 20, 35, 60, and 140 cm) at three-week intervals throughout the experiment. For PIC and POC, we could do it only at the end of the experiment (because of constraints in sampling we could not harvest soil samples at the beginning of the experiment). So for these two measurements, if the treatment resulted in more C in a given pool, we would measure a higher pool size in the basalt samples. At the end of the experiment, we collected 3 randomly taken soil samples per unit and dried them overnight in an oven at 60°C. Then, PIC was measured as total inorganic carbon (carbonates) in soil sample after drying, and was measured by measuring CO₂ formation after acidifying soil sample with phosphoric acid in TOC/TN analyser. Finally, POC was measured as total organic carbon on a TOC/TN analyser on dried soil samples.



195 2.12 C isotope analyses

We aimed to rule out the possibility that the basalt directly reacted with CO₂ from the atmospheric pool rather than with CO₂ derived from soil respiration. This process can be effectively traced using isotopic analysis, as the CO₂ supplied by the ecotron's control system has a distinctly negative δ¹³C signature. If atmospheric CO₂ were directly fixed by the basalt, it would result in a detectable shift toward more negative δ¹³C values in the soil carbon pool. With strong isotopically fractionating C-
 200 assimilation linked to photosynthesis, it is possible to trace and differentiate the plant-derived C, serving as a substrate to the soil organic carbon (SOC, δ¹³C = - 27.0 ‰ vs. VPDB, see Figure S2) and being respired from CO₂-C, which might be directly adsorbed from the isotopically enriched signal being supplied into the ecotron via CO₂ tanks (-30 ‰ vs. VPDB). Thus, if the treatment with basalt would result in a shift of the isotopic ratio of the SOC towards the atmospheric value, this would be indicative of adsorption with further incorporation from this source into the SOC.

205 Soil samples were taken in September 2022, at the end of the experiment. They were dried (60°C, 24 h, atmospheric pressure) and subsequently milled using a ball mill (MM2, Retsch, Haan, Germany). Samples were then weighed into tin foil and measured against a lab standard (acetanilid, p.a., IVA Analysentechnik, Meerbusch, Germany) calibrated against international standards (IAEA CH-7 and IAEA CH-3, International Atomic Energy Agency, IAEA, Vienna, Austria) using an Elemental analyser (EA IsoLink CN, Thermo Fisher Scientific, Germany) connected via a continuous flow open split interface (ConFlo
 210 IV, Thermo Fisher Scientific, Bremen, Germany) to an isotope ratio mass spectrometer (DELTA V Advantage, Thermo Fisher Scientific, Bremen, Germany). All ¹³C/¹²C ratios are reported using the δ-notation against the internationally recognized ratio of Vienna Pee-Dee Belemnite (VPDB) and expressed in per mille (‰) (Coplen, 2011; McKinney et al., 1950):

$$\delta^{13}\text{C} = (\text{R}_{\text{sample}}/\text{R}_{\text{standard}} - 1)$$

where R represents the ratio of the heavier to the most abundant stable isotope of the corresponding element (e.g., R = ¹³C/¹²C),
 215 with ¹³R_{VPDB} = 0.0111802, as recorded in the software (Isodat 3, version 3.0.94.12, Thermo Fisher Scientific, Bremen, Germany).

2.13 Effect of treatment on soil CO₂ adsorption capacity

Finally, we investigated whether the observed increase in soil carbon in the basalt-amended macrocosms could be attributed to a purely physical adsorption mechanism. Silicate rock powders possess a high surface area and a crystalline structure capable



220 of adsorbing various gases (Ramos et al., 2022), and could, in principle, retain CO₂ from soil respiration in the gaseous phase. To test this, we conducted a series of experiments on soil samples from the macrocosms to evaluate their CO₂ adsorption properties. We investigated whether the observed increase in soil carbon in the basalt-amended macrocosms could be attributed to a purely physical adsorption mechanism. We validated this assumption by conducting additional continuous-flow CO₂ adsorption experiments using a humid CO₂/Ar gas mixture (RH = 100%, CO₂ concentration = 28.5 vol%).

225 **2.14 Microbial metabolic activity**

Microbial metabolic activity in soil was measured to compare basalt and control treatments and to help interpret soil C fluxes. The FDA (Fluorescein Diacetate) assay, which estimates microbial activity by measuring the conversion of fluorescein diacetate to fluorescein by microbial enzymes, was used (Adam and Duncan 2001). For 13 consecutive days in May 2022, three soil samples (1 cm diameter, 10 cm deep) were collected per macrocosm, stored at -19°C, sieved, and aliquoted to 0.1
 230 grams dry weight. Samples were incubated in sodium phosphate buffer with FDA solution at 30°C for 16 hours. After dilution, absorbance was measured at 490 nm, and values were converted to moles of substrate using a calibration curve.

2.15 Statistics

Data in Figure 1 summarize total carbon fluxes during the growing season, corresponding to single-time-point biomass measurements taken at harvest. However, hourly CO₂-C net flux recordings enabled finer-scale analysis, so we evaluated
 235 treatment impacts on daily CO₂-C net flux using a linear mixed-effects model incorporating treatment, ecotron unit, and day as factors. Each flux is associated with its own standard deviation. Two components, “plantC” and “leachateC” were estimated through an internal bootstrap procedure to account for uncertainty arising from stem density estimates, the C content of plant organs (20% to 60%)(plantC) and the amount of water sampled per sampling event (5 to 15l). To propagate uncertainty across the entire soil C net flux calculation, we used a bootstrapping approach (n = 10,000) to generate empirical distributions of the
 240 soil C net flux for each treatment. We then applied a bootstrap hypothesis test to evaluate the observed treatment effect against a null distribution assuming no treatment difference. Additional analyses employed similar modeling approaches for other variables including organ-specific biomass, stem density, soil C isotopes, and inorganic C in soil water. For inorganic C in the soil solution (DIC), as well as Ca and Mg in the soil solution, as the dataset was gappy, but also more structured from the fixed



variables depth and date, we used a different bootstrapping approach. We generated empirical distributions of the concentration
 245 of the element (iC, Ca or Mg) in soil solution at the unit level (in order to keep the structure induced by depth and date). We
 then ran a generalized linear model with treatment, depth and their interaction as fixed variables and unit and date as random
 variables, and computed the average estimate and p-value of the effect of treatment across all iterations ($n = 1,000$). Statistics
 were done in R (R core team, 2019) using nlme (Pinheiro et al., 2023), dplyr (Wickham et al., 2023), lubridate (Grolemund &
 Wickham, 2011) and vegan (Oksanen et al., 2013) packages.

250 **3 Results**

3.1 Climatic conditions

The spring began unusually cold with night frosts and temperatures below 5°C in early March, rapidly transitioning to warmth
 in April (20°C maxima) and subsequent heatwaves in May (30°C). Summer remained consistently warm, punctuated by a
 late-June heatwave. Rainfall was frequent yet light (<15mm/day) throughout most of the growing season except for brief
 255 periods of drought and heavy rains in mid-May and early June. Consequently, soil moisture fluctuated between extremes: rapid
 depletion to ~5% during the May heatwave, short-lived recoveries exceeding 10%, and sustained lows (<5%) throughout
 summer (Figure S1).

3.2 Effect of basalt amendment on ecosystem C fluxes

The largest input flux, by far, came from net CO₂ exchange (366 to 457 gC/m² depending on the treatment), which was almost
 260 two orders of magnitude larger than all other fluxes (1 to 7 gC/m² depending on the flux and the treatment) (Figure 1). The
 crop system was a net CH₄ sink throughout the experiment. The macrocosm was a net C sink in both treatments (456 gC/m²
 and 361 gC/m² in basalt and control units, respectively).

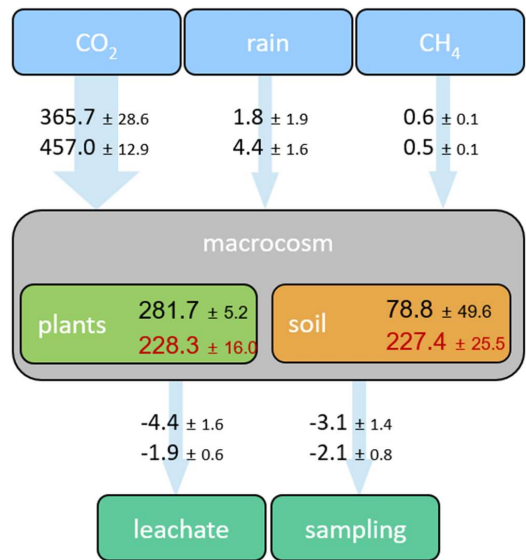


Figure 1. Measured net C fluxes and pools to the macrocosms in both treatments (black: control, red: basalt), in g/m² aggregated for the whole growing season, and averaged per treatment (n=3; +/- standard error). The total macrocosm C pools entailed plant and soil C pools, plant C pool being measured directly and soil C pool calculated as a difference between total macrocosm C pool and the plant pool. Negative values indicate a net loss of C from the ecosystem, and positive values indicate net C gain in the ecosystem. Note that the sampling pool corresponds to the soil pore water sampling occurring every 3 weeks.

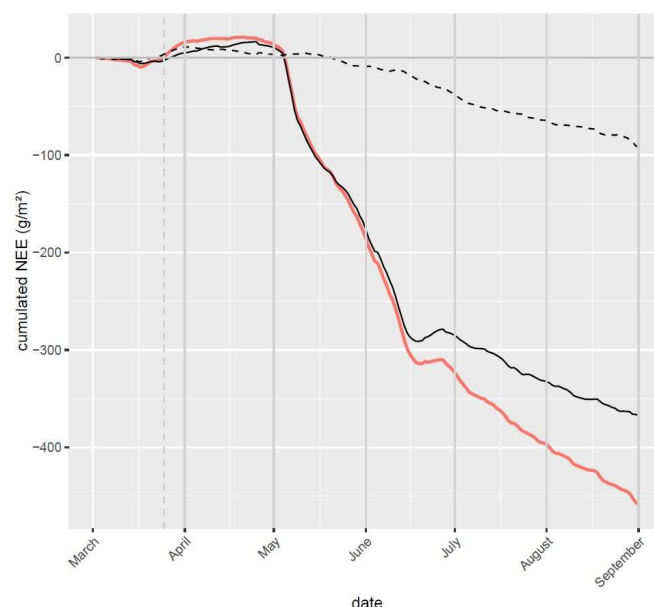
We then partitioned the sequestered carbon (C) within each macrocosm into two primary pools: plant biomass and soil. Plant biomass was significantly lower in the EW treatment (228 g C/m² vs. 282 g C/m² in the control) (Figure S3). Notably, the estimated root biomass was relatively low, comprising only 6% of total plant dry mass (Figure S4), whereas values reported in the literature typically range between 15% and 30% for oat (Gao et al., 2019). Despite thorough sampling, it is possible that some root biomass remained in the soil, potentially leading to an underestimation. Based on this discrepancy, we estimated that root biomass may have been underestimated by 10–59 g C/m².

Approximately 40% of the total fixed C was allocated to the soil pool (153 ± 41 g C/m² across treatments) (Figure 1). The basalt treatment led to a substantial and statistically significant increase in soil C sequestration, with values 2.9 times higher (227 ± 26 g C/m²) than in the control (79 ± 50 g C/m²), corresponding to a difference of 149 g C/m² (p = 0, bootstrap test; note that the bootstrapped difference in mean values was 155 g C/m², see Figure S5). These results were robust to assumptions in



280 pore water sampling flux (5 to 15 L per sampling date; $p = 0$ and 149 to 150 g C/m² in soil sequestration) and plant C content (20% to 60%; $p = 0$ and 133 to 197 g C/m² in soil C sequestration). Immediately after applying basalt, elevated CO₂ emissions occurred likely due to soil disturbance (Figure 2). Subsequently, both treatments exhibited comparable CO₂ dynamics until mid-May/mid-June when differences emerged, accelerating sharply during the June/July heatwave before stabilizing later in the season (Figure 2). These trends coincided with rising soil temperatures (~20°C). Despite lacking separation of plant vs.

285 soil-derived carbon, negligible variations in final biomass suggest the observed patterns reflect differential soil carbon sequestration. Notably, changes in net carbon balance were strongly inversely linked to soil temperature (Figure S6) rather than moisture.



290 **Figure 2.** Effect of the EW treatment on the dynamics of the C balance of the system. Black: control, Red: basalt treatment; dashed black line: difference between the two treatments; vertical dashed grey line: date of the basalt amendment. The NEE has been estimated per hour and per unit (three units per treatment) using a model accounting for CO₂ corrections, temperature and pressure, and aggregated per day (sum) and then per treatment (average) and cumulated throughout the growing season. We also computed the difference between the average in the two treatments (dashed line).



3.3 Soil carbonates in the basalt-treated macrocosms

No significant differences in inorganic carbon concentrations were observed between treatments at any depth, even when using
 295 bootstrap approach to address the gappy nature of the dataset (estimate of treatment “control”= -0.72 ± 1.49 , average p-
 value=0.43) with both inorganic and organic C levels remaining below 0.2 gC/m^2 ($1\text{--}5 \text{ mgC/L}$) (Table 1). To adjust for varying
 relevance of inorganic carbon increases across depths, we normalized values according to the respective soil column volumes
 and moisture contents. Specifically, an increment of 10 mg/L in shallow layers (short columns, lower moisture) contributed
 less significantly to the overall budget compared to deeper strata (longer columns, higher moisture). After multiplying
 300 inorganic C values by adjusted soil volumes and moisture, bootstrapping yielded statistically nonsignificant results. (estimate
 of treatment “control”= $9.7 \pm 16.5 \text{ mgC/L}$, average p-value=0.43). Additionally, we re-ran the bootstrap analysis focusing
 exclusively on post-May 17th data, given the emergence of significant basalt-treatment effects on Net Ecosystem Exchange
 (NEE) thereafter. Nevertheless, this refined analysis still failed to reveal any discernible differences in dissolved inorganic
 carbon among treatments (estimate of treatment “control”= 21.2 ± 23.3 , average p-value=0.55). An alternate explanation
 305 posits that carbonates might have initially formed in the soil but later degassed as CO_2 during sample storage prior to analysis.
 Under this scenario, evidence of carbonate formation should manifest as elevated concentrations of divalent cations (Ca^{2+} ,
 Mg^{2+}), resulting from silicate mineral dissolution. However, no significant treatment-related changes in calcium or magnesium
 concentrations were detected in soil pore waters (for Ca: estimate of treatment “control”= -3.17 ± 3.28 , average p-value=0.28;
 for Mg: estimate of treatment “control”= 0.14 ± 1.76 , average p-value=0.59, Figure S7).
 310 One possible explanation for the absence of dissolved inorganic carbon is the precipitation of carbonate ions. Such carbonates
 would then be present as solid-phase PIC rather than in solution. To investigate this, we measured PIC in soil samples and
 found no significant differences between treatments ($222 \pm 13 \text{ g/m}^2$ in the basalt-amended plots vs. $214 \pm 3 \text{ g/m}^2$ in controls;
 t-test, $p = 0.28$) (Table 2, Figure S8).

315



Table 1. Inorganic carbon concentration of soil water samples taken by suction cups. The suction cups were installed at 5 different depths, and set at a tension of -150 HPa until 35cm deep and -50 HPa below. Soil water was sampled every 3 weeks and analysed for TOC and inorganic C.

unit	depth (cm)	15/03	5/04	26/04	17/05	7/06	28/06	19/07	9/08	30/08
1	10		15,6	8,8		3,8	11,2	11,5		
	20		4,8	4,9	4,4	4,5				
	35		1,6	1,6	1,5	1,2	4,3	1,5		4,5
	60		1,3	4,5	0,7	0,6	4,3			
	140						14,8			
3	10		3,2	7,8					5,0	
	20							3,8	4,0	
	35		1,5	1,5	0,7	4,5				4,4
	60		0,9	1,2	0,7	1,3	1,0			
	140	1,1		0,9	0,8	0,8	0,9			
4	10			4,3	3,9	1,0	3,0			
	20		4,5	4,3	3,5	1,7		4,0		4,0
	35		4,5	3,4	1,4	5,3				
	60									
	140								7,2	
Basalt		1,1	4,2	3,9	2,0	2,5	5,6	5,2	5,4	4,3
6	10					1,9				
	20					6,2				
	35		4,7	0,8	3,6			3,6	4,9	4,3
	60	0,9	0,9	0,8	0,7	0,9	0,6			
	140	0,9	0,9	0,8	0,7	0,9	0,8			
10	10				3,9	5,5				
	20		4,8	5,4	3,9		4,1		4,3	4,0
	35	1,2	1,5	1,6	1,2	5,0		3,9	4,2	
	60	1,3	1,5	1,3	0,7	1,4				
	140	1,9	1,9	0,9	1,5	3,3	5,0			
11	10		1,8	4,0	4,1	6,4				
	20		5,1				4,8			
	35					0,8				
	60		1,0	0,8						
	140									
Control		1,2	2,4	1,8	2,3	3,5	3,1	3,8	4,5	4,2

- 320 **Table 2. Size of C pools in the topsoil (0 - 20 cm) of the macrocosms, in gC/m² measured at the end of the growing season. PIC:**
 Particulate Inorganic Carbon, measured as soil dry mass in the topsoil (0-20 cm) samples. POC: Particulate Organic Carbon,
 measured as mmol/gDW in 20 cm deep soil samples. DIC: Dissolved Inorganic Carbon, measured as total C minus total organic C
 concentration (mg/l) in 10 and 20 cm soil water samples collected throughout the growing season by the lysimeter suction cups.
 325 **DOC: Dissolved Organic Carbon, measured as organic C concentration (mg/l) in 10 and 20 cm soil water samples collected**
 throughout the growing season by the lysimeter suction cups. All four parameters were converted to gC m⁻² in the top 20 cm by
 accounting for a density of 1.3, 12g/mol C, and 10 % soil moisture for DIC and DOC (average moisture in the top 20 cm of soil across
 the growing season).

treatment	Basalt		control	
	average	standard error	average	standard error
Soil PIC	222	13	214	3
Soil POC	3713	720	5086	921
Soil DIC	0.03	0.03	<0.01	<0.01
Soil DOC	0.13	0.03	0.10	0.06



3.4 Contribution of soil C in the gas phase: CO₂ adsorbed to the basalt powder

Thermogravimetric analysis revealed that the presence of basalt approximately doubled the soil's CO₂ adsorption capacity.

330 However, desorption tests confirmed that the CO₂ was held through weak, reversible physical adsorption, with rates of 0.170 wt% and 0.036 wt% for basalt-amended and control soils, respectively (Table S2). These numbers were negligible in comparison with the other estimated C fluxes.

3.5 Direct fixation of atmospheric CO₂ by basalt

Finally, we aimed to rule out the possibility that the basalt directly reacted with CO₂ from the atmospheric pool rather than with CO₂ derived from soil respiration. This process can be effectively traced using isotopic analysis, as the CO₂ supplied by the ecotron's control system has a distinctly negative $\delta^{13}\text{C}$ signature. If atmospheric CO₂ were directly fixed by the basalt, it would result in a detectable shift toward more negative $\delta^{13}\text{C}$ values in the soil carbon pool. However, we observed no such isotopic shift, suggesting that direct atmospheric CO₂ fixation by the basalt was negligible. Although isotopic variability was slightly higher in the basalt treatment, the overall pattern did not support significant atmospheric CO₂ incorporation (Figure

340 S2).

3.6 Microbial activity

Microbial activity was significantly higher (+32% on average, $p=0.005$) in basalt-treated soils midway through the growing season (Figure S9).

4 Discussion

345 4.1 ERW enhanced soil C pools substantially

Our study demonstrated a 2.9-fold increase in carbon sequestration under ERW treatment, adding 150 g/m² to the soil's carbon stock over one growing season, despite initial CO₂ emissions triggered by soil disturbance. Robust sensitivity analyses supported this finding. Relative to baseline conditions, and based on the following reasonable assumptions (macrocosm volume of 4.4 m³, of a mean bulk density of 1.6 kg/dm³, in a 7 ton dry soil mass, and a mean total organic carbon (TOC) content of



0.7% (1.9% in the top 20 cm, 0.5% below, down to 140 cm depth)) this equated to a 1.2% boost in total soil carbon, far surpassing the "4 per 1000" initiative's goal for mitigating climate change (Minasny et al., 2017). This corresponds to an increase of 0.17 tons of carbon sequestered per tonne of basalt amendment applied (equivalent to 10 tons per hectare), falling within the range observed in other ERW field trials (Ramos et al., 2022; Swoboda et al., 2022). However, most studies cited in these reviews involved amending with non-basaltic rocks and assessed performance over multi-year timescales. A more analogous study by Kelland et al. (2020) similarly reported equivalent levels of carbon sequestration using basalt, along with a comparable fold-increase versus controls (fourfold instead of threefold here). However, this outcome was achieved under a considerably larger amendment dosage (100 tons per hectare). Alternatively, carbon sequestration rates nearing 2 tons per hectare were realized within a single year using equal amendment quantities (10 tons per hectare), though this involved utilizing a more chemically reactive substance—olivine—as opposed to basalt (Dietzen et al., 2019). Thus, the quantity of carbon sequestered in our investigation notably exceeds typical expectations given the amendment type and dosage. Let us explore potential influences on the observed carbon sequestration rates in our experiment. Firstly, the ambient CO₂ concentration was artificially raised by approximately 200 ppm as part of a broader research program investigating various amendments' responses to projected climatic conditions (Rineau et al., 2024; Schroeder et al., 2021). Enhanced CO₂ levels are known to stimulate both weathering rates and CO₂ uptake via electrochemically-driven reactions (Amann et al., 2022). Additionally, elevated atmospheric CO₂ enhances crop biomass production (Kimball, 2016), amplifying carbon inputs into the soil via root exudation. Secondly, we also measured significantly higher microbial activity in basalt-amended soils, mirroring findings by Li et al. (2020), who reported a 33% increase in microbial activity following enriched rock-dust applications in orchards. Such higher microbial activity can lead to localized elevations in CO₂ concentrations adjacent to amendment sites. Thirdly, soil structures were preserved in our macrocosms, unlike the column-based study by Kelland et al. (2020), where extensive soil sieving may have disrupted native soil structure, fauna and mycelium networks, thus emphasizing the importance of soil organisms in sequestration processes. Fourthly, however, and most importantly, the degree of carbon sequestration achieved—approximately 17% of the applied basalt amendment within a single growing season—is sevenfold higher than comparable studies using basalt (Kelland et al., 2020). Remarkably, this figure slightly exceeds the theoretically achievable limit of converting applied basalt into entirely carbonates (144 kg/ha for a 10 t/ha amendment). Hence, either complete



375 transformation of the amendment occurred exceptionally swiftly within three months, which appears improbable based on
existing literature (Kelland et al., 2020), or alternative mechanisms contributing to soil carbon sequestration must be
considered.

4.2 No evidence for inorganic C formation

This high C sequestration was moreover not followed by noticeable increases in soil inorganic C pools, contrary to expectations
380 with ERW. The experimental design did not allow us to take soil samples before the experiment and therefore to understand
how different C pools were affected by the treatment, we can only compare the size of the pools in both treatments.

We did not detect any significant increase in soil inorganic C, whether in solution or as particulate inorganic C. We therefore
have no evidence of carbonate ion formation, which is the central premise of ERW. The sequestered carbon was not detected
in plant biomass or as gas trapped within amendment pores either. The most surprising is the lack of dissolved carbonates in
385 soil solutions. Due to gaps in soil-water chemistry data (particularly scarce samples from drier upper layers), a comprehensive
carbon budget could not be constructed. Bootstrap analyzes indicated no intertreatment disparities in dissolved inorganic
carbon, nor any evidence of ERW-relevant Ca/Mg ion leaching. Nevertheless, two plausible explanations remain for why
bicarbonates might have gone undetected: first, potential sub-surface bicarbonate formation beyond our 20 cm measurement
depth, although carbonate genesis typically initiates closer to the surface; second, extremely gradual topsoil carbonate
390 formation rates, particularly during the dry June–July period when most soil water was unavailable for sampling. While our
current data provide no support for ERW-mediated reactions, we acknowledge methodological limitations prevent definitive
conclusions regarding their occurrence.

4.3 Extra mechanisms of C sequestration

Nevertheless, the proposed bias fails to adequately explain the observed extent of soil carbon sequestration. Complete
395 dissolution of the amendment through ERW within such a brief timeframe is implausible and insufficient to account for the
entirety of sequestration. Temporal dynamics of sequestration merit particular scrutiny: initiation coincided with topsoil
temperatures crossing a 20°C threshold, occurring comparatively late in the growing season when significant plant biomass



had already developed. Intensification during a concurrent heatwave underscores thermal dependency. Limited soil moisture throughout the season reduced moisture-related constraints on EW reactions (Guo et al., 2023).

400 We speculate that under the amendment, root exudates interact with fine particles of the silicate rock, creating organo-mineral complexes that are making C recalcitrant. Indeed, weathering products of basalt are known to undergo such reaction, and these results could partially illustrate the synergy between EW and SOM accrual described by (Buss et al., 2024), despite the absence of clear evidence of EW in our study. Indeed it has been shown that mineral-associated organic matter (MAOM) is a strong stabilizing factor for organic matter (Cotrufo et al., 2012). However MAOM formation cannot account for all of the
405 sequestration observed, as it is dependent of formation of secondary minerals from ERW, especially since basalt is known to be more reactive for ERW than for SOM accrual (Buss et al., 2024).

Alternatively, basalt may stimulate root exudation, facilitating interactions with pre-existing soil constituents to produce particulate organic carbon (POM) or additional MAOM. However, root exudates constitute merely 5–10% of assimilated carbon (yielding a maximum contribution of 0.1–0.2 t/ha), which would contribute to only a fraction of the excess
410 sequestration. However, formation of aggregates due to abiotic process of Ca and Mg provided by the basalt also played a significant role in the sequestration potential, as was observed before by (Buss et al., 2024), especially since the basalt used in our study was 3 times richer in these elements than in that publication. However, according to the same study, plant should reduce this protection through plant exudates solubilising Ca and Mg (Buss et al., 2023). Root biomass was very low, suggesting that plant reduction of soil aggregation was limited. However, we did not observe clear solubilization of Ca and
415 Mg; but we cannot rule out this process for the same reason of low sampling intensity from end of May onwards. It is therefore possible that organic matter decomposition products may play a role as well there, and that labile organic C initially present in the soil and/or resulting from the decomposition substantially contributes to this very high sequestration rate.

5 Conclusion

Our results demonstrate that basalt addition enhances the crop ecosystem's role as a carbon sink, increasing soil carbon
420 sequestration by a factor of 3 over the growing season. It turned the macrocosms from low (0.5 tC/Ha)) to significant (1.5 tC/Ha) C sinks despite initial C loss due to soil disturbance when applying the treatment. We had no evidence that the ERW



reaction took place, but we cannot rule out that it happened because our experimental design did not allow for complete budget of dissolved inorganic C. However, the amount of sequestered C is too high to be explained only by ERW. We conclude that enhanced weathering led to substantial C accrual, possibly stimulating the formation of both mineral-associated and
425 particulate organic matter. Therefore, we advise caution in the widespread application of enhanced weathering until its effects on soil health and organic matter transformation are better understood.

Author contribution

FR, MM, VP, PS, WS, BS, RZ and EL contributed to conceptualization, methodology and validation. FR, AHF, JG, KG, AL, DK, MMD, BP, JP, TP, TR, XS, HV, JV, and MZ contributed to analysis and data curation. FR wrote the original draft. FR,
430 AHF, JG, AL, DK, MM, VP, PS, WS, BR, HV, JV, RZ and EL reviewed and edited the draft. FR, AHF, JG, AL, DK, TP, HV, JV contributed to the figures. FR, MM, VP, PS, WS, BR, RZ and EL contributed to the funding acquisition.

Competing interests

The authors declare that they have no conflict of interest.

Acknowledgements

435 We thank Carina Bauer and Petra Eckert of the Centre of Stable Isotope Research in Ecology and Biogeochemistry (BayCenSI, www.censi.uni-bayreuth.de) for their skilful technical assistance, and we thank Maria Sharro for assistance with graphical design of figures used in the manuscript. The authors used artificial intelligence tools (ChatGPT) to assist with English language editing of the manuscript.

Financial support

440 The study was supported by the FACCE-SURPLUS project BiofoodonMars, and financed by the Flemish Fonds voor Wetenschappelijk Onderzoek (FWO). D.I.K. and J.V.V. acknowledge the support by the Ministry of Science and Higher Education of the Russian Federation for Boreskov Institute of Catalysis (project no. FWUR-2024-0032 and FWUR-2024-0036)



445 References

- Amann T, Hartmann J, Hellmann R, Pedrosa ET and Malik A (2022) Enhanced weathering potentials—the role of in situ CO₂ and grain size distribution. *Front. Clim.* 4:929268. doi: 10.3389/fclim.2022.929268
- Beerling, D. J., Kantzas, E. P., Lomas, M. R., Wade, P., Eufrazio, R. M., Renforth, P., Sarkar, B., Andrews, M. G., James, R. H., Pearce, C. R., Mercure, J. F., Pollitt, H., Holden, P. B., Edwards, N. R., Khanna, M., Koh, L., Quegan, S., Pidgeon, N. F., Janssens, I. A., ... Banwart, S. A. (2020). Potential for large-scale CO₂ removal via enhanced rock weathering with croplands. *Nature*, 583(7815), 242–248. <https://doi.org/10.1038/s41586-020-2448-9>
- 450 Beerling, D. J., Leake, J. R., Long, S. P., Scholes, J. D., Ton, J., Nelson, P. N., Bird, M., Kantzas, E., Taylor, L. L., Sarkar, B., Kelland, M., Delucia, E., Kantola, I., Müller, C., Rau, G. H., & Hansen, J. (2018). Climate , Food and Soil Security. *Nature Plants*, 4(March), 138–147. <http://dx.doi.org/10.1038/s41477-018-0108-y>
- 455 Buss, W., Hasemer, H., Ferguson, S., & Borevitz, J. (2024). Stabilisation of soil organic matter with rock dust partially counteracted by plants. *Global Change Biology*, 30, e17052. <https://doi.org/10.1111/gcb.17052>
- Buss, W., Hasemer, H., Sokol, N.W. et al. Applying minerals to soil to draw down atmospheric carbon dioxide through synergistic organic and inorganic pathways. *Commun Earth Environ* 5, 602 (2024). <https://doi.org/10.1038/s43247-024-01771-3>
- 460 Cipolla, G., Calabrese, S., Noto, L. V., & Porporato, A. (2021). The role of hydrology on enhanced weathering for carbon sequestration II. From hydroclimatic scenarios to carbon-sequestration efficiencies. *Advances in Water Resources*, 154(May), 103949. <https://doi.org/10.1016/j.advwatres.2021.103949>
- Clobert, J., Chanzy, A., Galliard, J. Le, Chabbi, A., Greiveldinger, L., Caquet, T., Loreau, M., & Mougin, C. (2018). How to Integrate Experimental Research Approaches in Ecological and Environmental Studies : AnaEE France as an Example. *Frontiers in Ecology and Evolution*, 6(April). <https://doi.org/10.3389/fevo.2018.00043>
- 465 Coplen, T. . (2011). Guidelines and recommended terms for expression of stable-isotope-ratio and gas-ratio measurement results. *Rapid Commun. Mass Spectrom.*, 25, 2538–2560. <https://doi.org/https://doi.org/10.1002/rcm.5129>
- Cotrufo, M. F., Wallenstein, M. D., & Boot, C. M. (2013). *The Microbial Efficiency-Matrix Stabilization (MEMS) framework integrates plant litter decomposition with soil organic matter stabilization : do labile plant inputs form stable soil*



- 470 *organic matter* ? 988–995. <https://doi.org/10.1111/gcb.12113>
- Dietzen, C., Harrison, R., & Michelsen-Correa S., 2019. Effectiveness of enhanced mineral weathering as a carbon sequestration tool and alternative to agricultural lime: An incubation experiment. *International Journal of Greenhouse Gas Control*, 74(July 2018), pp251–258. <https://doi.org/10.1016/j.ijggc.2018.05.007>
- Dietzen, C., & Rosing, M. T. (2023). Quantification of CO₂ uptake by enhanced weathering of silicate minerals applied to
 475 acidic soils. *International Journal of Greenhouse Gas Control*, 125(June 2022), 103872. <https://doi.org/10.1016/j.ijggc.2023.103872>
- Gadd, G. M., Rhee, Y. J., Stephenson, K., & Wei, Z. (2012). Geomycology: Metals, actinides and biominerals. *Environmental Microbiology Reports*, 4(3), 270–296. <https://doi.org/10.1111/j.1758-2229.2011.00283.x>
- Gao, K., Yu, Y.F., Xia, Z.T. et al. Response of height, dry matter accumulation and partitioning of oat (*Avena sativa* L.) to
 480 planting density and nitrogen in Horqin Sandy Land. *Sci Rep* 9, 7961 (2019). <https://doi.org/10.1038/s41598-019-44501-y>
- Grolemund, G., & Wickham, H. (2011). Dates and Times Made Easy with lubridate. *Journal of Statistical Software*, 40(3), 1–25. <https://www.jstatsoft.org/v40/i03/>
- Guo, F., Wang, Y., Zhu, H., Zhang, C., Sun, H., Fang, Z., Yang, J., Zhang, L., Mu, Y., Man, Y. B., & Wu, F. (2023). Crop
 485 productivity and soil inorganic carbon change mediated by enhanced rock weathering in farmland: A comparative field analysis of multi-agroclimatic regions in central China. *Agricultural Systems*, 210(May), 103691. <https://doi.org/10.1016/j.agsy.2023.103691>
- Hannes, M., Wollschläger, U., Schrader, F., Durner, W., Gebler, S., Pütz, T., Fank, J., Von Unold, G., & Vogel, H. J. (2015). A comprehensive filtering scheme for high-resolution estimation of the water balance components from high-precision
 490 lysimeters. *Hydrology and Earth System Sciences*, 19(8), 3405–3418. <https://doi.org/10.5194/hess-19-3405-2015>
- Holzer, I. O., Nocco, M. A., & Houlton, B. Z. (2023). Direct evidence for atmospheric carbon dioxide removal via enhanced weathering in cropland soil. *Environmental Research Communications*, 5(10). <https://doi.org/10.1088/2515-7620/acfd89>
- IPCC. (2014). Climate Change 2014 Synthesis Report: Summary Chapter for Policymakers. *Ippc*, 31.



- 495 <https://doi.org/10.1017/CBO9781107415324>
- Kallenbach, C., & Grandy, A. S. (2011). Controls over soil microbial biomass responses to carbon amendments in agricultural systems : A meta-analysis. *"Agriculture, Ecosystems and Environment,"* 144(1), 241–252.
<https://doi.org/10.1016/j.agee.2011.08.020>
- Kantola, I. B., Blanc-Betes, E., Masters, M. D., Chang, E., Marklein, A., Moore, C. E., von Haden, A., Bernacchi, C. J., Wolf,
 500 A., Epihov, D. Z., Beerling, D. J., & DeLucia, E. H. (2023). Improved net carbon budgets in the US Midwest through direct measured impacts of enhanced weathering. *Global Change Biology, May*, 7012–7028.
<https://doi.org/10.1111/gcb.16903>
- Kelland ME, Wade PW, Lewis AL, et al. Increased yield and CO2 sequestration potential with the C4 cereal *Sorghum bicolor* cultivated in basaltic rock dust-amended agricultural soil. *Glob Change Biol.* 2020; 26: 3658–3676.
 505 <https://doi.org/10.1111/gcb.15089>
- Kimball BA, 2016. Crop responses to elevated CO2 and interactions with H2O, N, and temperature. *Current Opinion in Plant Biology*, 31:36–43. <https://doi.org/10.1016/j.pbi.2016.03.006>
- Li, J., Mavrodi, D. V., & Dong, Y. (2020). Effect of rock dust-amended compost on the soil properties, soil microbial activity, and fruit production in an apple orchard from the Jiangsu province of China. *Archives of Agronomy and Soil Science*,
 510 67(10), 1313–1326. <https://doi.org/10.1080/03650340.2020.1795136>
- McKinney, C. R., McCrea, J. M., Epstein, S., Allen, H. A., & Urey, H. C. (1950). Improvements in mass spectrometers for the measurement of small differences in isotope abundance ratios. *Rev. Sci. Instrum.*, 21, 724–730.
<https://doi.org/https://doi.org/10.1063/1.1745698>
- Minasny, B., Malone, B. P., McBratney, A. B., Angers, D. A., Arrouays, D., Chambers, A., Chaplot, V., Chen, Z. S., Cheng,
 515 K., Das, B. S., Field, D. J., Gimona, A., Hedley, C. B., Hong, S. Y., Mandal, B., Marchant, B. P., Martin, M., McConkey, B. G., Mulder, V. L., ... Winowiecki, L. (2017). Soil carbon 4 per mille. *Geoderma*, 292, 59–86.
<https://doi.org/10.1016/j.geoderma.2017.01.002>
- Oksanen, J., Blanchet, F. G., Kindt, R., Legendre, P., Minchin, P. R., O'Hara, R. B., Simpson, G. L., Solymos, P., Henry, M., Stevens, H., & Wagner, H. (2013). *Vegan: Community Ecology Package. R package version 2.0-10.*



- 520 Peters, A., Groh, J., Schrader, F., Durner, W., Vereecken, H., & Pütz, T. (2017). Towards an unbiased filter routine to determine precipitation and evapotranspiration from high precision lysimeter measurements. *Journal of Hydrology*, 549, 731–740. <https://doi.org/10.1016/j.jhydrol.2017.04.015>
- Pinheiro, J., Bates, D., & R coreTeam. (2023). *nlme: Linear and Nonlinear Mixed Effects Models* (p. R package version 3.1-162, <https://CRAN.R-project.org/>).
- 525 R core team. (2019). *R: A language and environment for statistical computing*. R Foundation for Statistical Computing. <https://www.r-project.org/>.
- Ramos, C. G., Hower, J. C., Blanco, E., Oliveira, M. L. S., & Theodoro, S. H. (2022). Possibilities of using silicate rock powder: An overview. *Geoscience Frontiers*, 13(1), 101185. <https://doi.org/10.1016/j.gsf.2021.101185>
- Rijnders, J., Vicca, S., Struyf, E., Amann, T., Hartmann, J., Meire, P., Janssens, I., & Schoelynck, J. (2023). The effects of
 530 dunite fertilization on growth and elemental composition of barley and wheat differ with dunite grain size and rainfall regimes. *Frontiers in Environmental Science*, 11(August), 1–19. <https://doi.org/10.3389/fenvs.2023.1172621>
- Rineau, F., Groh, J., Claes, J., Grosjean, K., Mench, M., Moreno-druet, M., Povilaitis, V., Pütz, T., Szulc, W., Thijs, S., Vandenberght, J., Vangronsveld, J., Vereecken, H., Verhaege, K., Zydels, R., & Loit, E. (2024). Limited effects of crop foliar Si fertilization on a marginal soil under a future climate scenario. *Heliyon*, 10(December 2023), 1–12.
 535 <https://doi.org/10.1016/j.heliyon.2023.e23882>
- Rineau, F., Malina, R., Beenaerts, N., Arnauts, N., Bardgett, R. D., Berg, M. P., Boerema, A., Bruckers, L., Clerinx, J., Davin, E. L., De Boeck, H. J., De Dobbelaer, T., Dondini, M., De Laender, F., Ellers, J., Franken, O., Gilbert, L., Gudmundsson, L., Janssens, I. A., ... Vangronsveld, J. (2019). Towards more predictive and interdisciplinary climate change ecosystem experiments. *Nature Climate Change*, 9(11), 809–816. <https://doi.org/10.1038/s41558-019-0609-3>
- 540 Roy, J., Rineau, F., De Boeck, H. J., Nijs, I., Pütz, T., Abiven, S., Arnone, J. A., Barton, C. V. M., Beenaerts, N., Brüggemann, N., Dainese, M., Domisch, T., Eisenhauer, N., Garré, S., Gebler, A., Ghirardo, A., Jasoni, R. L., Kowalchuk, G., Landais, D., ... Milcu, A. (2021). Ecotrons: Powerful and versatile ecosystem analysers for ecology, agronomy and environmental science. *Global Change Biology, Online first*, 1–21. <https://doi.org/10.1111/gcb.15471>
- Sun, Z., Wu, S., Zhu, B., Zhang, Y., Bol, R., Chen, Q., & Meng, F. (2019). *Variation of 13 C and 15 N enrichments in different*



- 545 *plant components of labeled winter wheat (Triticum aestivum L.)*. 1–22. <https://doi.org/10.7717/peerj.7738>
- Swoboda, P., Döring, T. F., & Hamer, M. (2022). Remineralizing soils? The agricultural usage of silicate rock powders: A review. *Science of the Total Environment*, 807. <https://doi.org/10.1016/j.scitotenv.2021.150976>
- Vanderkelen, I., Zschleischler, J., Gudmundsson, L., Keuler, K., Rineau, F., Beenaerts, N., Vangronsveld, J., & Thiery, W. (2019). A new approach for assessing climate change impacts in ecotron experiments. *Biogeosciences Discussions*, 1–
- 550 38. <https://doi.org/10.5194/bg-2019-267>
- Vienne, A., Poblador, S., Portillo-Estrada, M., Hartmann, J., Ijehon, S., Wade, P., & Vicca, S. (2022). Enhanced Weathering Using Basalt Rock Powder: Carbon Sequestration, Co-benefits and Risks in a Mesocosm Study With *Solanum tuberosum*. *Frontiers in Climate*, 4(May), 1–14. <https://doi.org/10.3389/fclim.2022.869456>
- Wickham, H., François, R., Henry, L., Müller, K., & Vaughan, D. (2023). *dplyr: A Grammar of Data Manipulation* (p.
- 555 <https://github.com/tidyverse/dplyr>).